The Astronomical Journal, 127:789–797, 2004 February

THE STELLAR CONTENT OF THE POLAR RINGS IN THE GALAXIES NGC 2685 AND NGC 4650A[1]

G. M. Karataeva,[2] I. O. Drozdovsky,[3] V. A. Hagen-Thorn,[2] and V. A. Yakovleva[2]
Astronomical Institute, St. Petersburg State University, Universitetskii pr. 28, St. Petersburg, 198504, Russia

and

N. A. Tikhonov[4] and O. A. Galazutdinova[4]
Special Astrophysical Observatory, Nizhnij Arkhyz, Zelenchukskaya, 369167, Karachaevo-Cherkesia, Russia
Received 2003 July 22; accepted 2003 October 22

ABSTRACT

We present the results of stellar photometry of polar ring galaxies NGC 2685 and NGC 4650A, using the archival data obtained with the *Hubble Space Telescope*'s Wide Field Planetary Camera 2. Polar rings of these galaxies were resolved into ~800 and ~430 stellar objects in the B, V, and I_C bands, a considerable part of which are blue supergiants located in the young stellar complexes. The stellar features in the CM diagrams are best represented by isochrones with metallicity $Z = 0.008$. The process of star formation in the polar rings of both galaxies was continuous, and the age of the youngest detected stars is about 9 Myr for NGC 2685 and 6.5 Myr for NGC 4650A.

Key words: galaxies: individual (NGC 2685, NGC 4650A) — galaxies: peculiar — galaxies: starburst — galaxies: stellar content

1. INTRODUCTION

Polar ring galaxies (PRGs) represent a rare class of peculiar objects containing a ring or annulus of gas, stars, and dust orbiting in a plane nearly perpendicular to the equatorial plane of the host galaxy. This unique geometry of PRGs gives an ideal opportunity to investigate the shape of their three-dimensional gravitational potential. Typically, the host galaxy looks like a galaxy of early morphological type but with some peculiarities in color and brightness distribution; sometimes these properties cause this component to appear more similar to a late-type object rather than to an S0 galaxy (e.g., Arnaboldi et al. 1995; Iodice et al. 2002). Recently, polar rings (PRs) have also been found around spiral galaxies NGC 660 (van Driel et al. 1995) and UGC 5600 (Karataeva et al. 2001). The main properties of PRs (compiled by Bournaud & Combes 2003) are similar to those of spiral arms: blue color, plenty of gas and dust, prominent star-forming regions, and disklike rotation.

According to the most popular point of view, PRGs are the result of galaxy interaction, ranging from simple gas accretion (e.g., Schweizer, Whitmore, & Rubin 1983) to complete merger (Bekki 1997). Both hypotheses are investigated in detail by Bournaud & Combes (2003). The authors conclude that both scenarios may explain the PRGs formation but the accretion one is preferable because some predictions relative to the merging scenario (such as the stellar halo around the PR) are not observed. Alternatively, PRs can represent the delayed inflows of primordial gas (e.g., Toomre 1977; Curir & Diaferio 1994).

Intensive studies of this strange objects have been started after publication of the atlas and catalog of PRGs and candidates for these objects (Whitmore et al. 1990), although strong emission lines in the spectra of PRs were detected before (e.g., Schechter & Gunn 1978; Schweizer et al. 1983). The presence of H II regions in the PRs of some nearby galaxies, such as NGC 2685 (Makarov, Reshetnikov, & Yakovleva 1989; Eskridge & Pogge 1997) and NGC 4650A (Eskridge & Pogge 1999), the optical colors and Hα luminosities of the rings (Reshetnikov & Combes 1994), as well as high IR fluxes of PRGs (Richter, Sackett, & Sparke 1994) suggest a presence of active star formation in PRs.

We present here a deep optical study based on *Hubble Space Telescope*'s (*HST*) Wide Field Planetary Camera 2 (WFPC2) archival data of the resolved stellar populations of two nearby PRGs, NGC 2685 ($D \sim 12.5$ Mpc) and NGC 4650A ($D \sim 35$ Mpc) ($H_0 = 75$ km s^{-1} Mpc^{-1}). Multicolor stellar photometry provides the opportunity to study directly the resolved stellar populations of different masses, ages, and chemical abundances. The analysis of the stellar distribution on color-magnitude diagrams (CMDs) is the most powerful way to investigate population fractions and their spatial variations, to estimate the galaxy distance, and to provide clues to its star formation history (e.g., Tolstoy 1999).

Both galaxies were included by Whitmore et al. (1990) in the group of most probable PRGs, "A," having two well-established orthogonal kinematic systems on the basis of optical (Sersic & Aguero 1972; Schechter & Gunn 1978; Schechter, Ulrich, & Boksenberg 1984) and radio–H I observations (Shane 1980). The important difference between these galaxies is that the PR of NGC 2685 is comparable in size to the host galaxy, while NGC 4650A has a PR extended out to more than two radii of the host galaxy.

NGC 2685 (Arp 336, also known as the Helix galaxy and the Spindle) has long been known as an unusual object (Sandage 1961). Figure 1 presents its image taken from the Digitized Sky Survey (DSS). Sandage (1961) pointed to the singularity of NGC 2685, and later Arp (1966) included

[1] Based on observations made with the NASA/ESO *Hubble Space Telescope*, obtained from the Space Telescope Science Institute, which is operated by the Association of Universities for Research in Astronomy, Inc., under NASA contract NAS 5-26555.
[2] Isaac Newton Institute of Chile, St. Petersburg Branch.
[3] Visiting Astronomer, *Spitzer* Science Center, MS 220-6, California Institute of Technology, Pasadena, CA 91125.
[4] Isaac Newton Institute of Chile, SAO Branch.

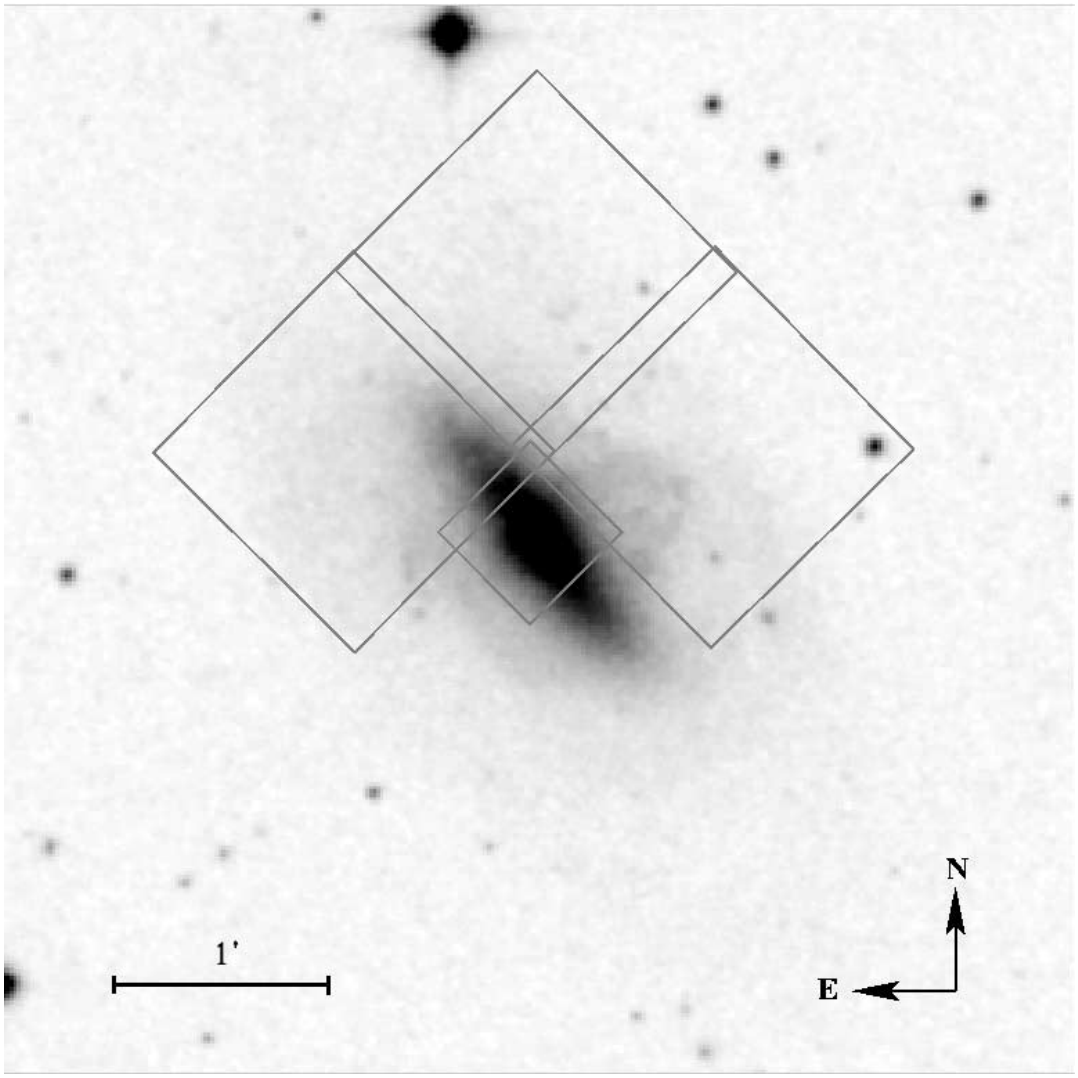

FIG. 1.—DSS $5' \times 5'$ image of NGC 2685 with the WFPC2 footprint overlaid

the galaxy in his atlas of peculiar galaxies. The main body of the galaxy having a spindle-like shape is twisted by luminous filaments (rings) traced by dark strips on the central galaxy. Deep images (see Sandage 1961) reveal an outer extended low-luminosity elliptical structure (outer ring) with position angle close to that of the galaxy major axis. The combination of photometric (Hagen-Thorn, Popov, & Yakovleva 1983; Makarov et al. 1989) and spectroscopic (Schechter & Gunn 1978) data shows that NGC 2685 is most likely an edge-on S0 galaxy with rings (helices) rotating approximately perpendicular to the main optical disk. The H I map (Shane 1980; Schinnerer & Scoville 2002) also shows an extended structure coincided with outer ring. One small, 16th magnitude galaxy lies within $10'$ (36 kpc in projection) of NGC 2685 and two more faint, small galaxies are within $20'$ (Richter et al. 1994). If they are not background objects, then the gas captured during the galactic interaction might produce such a peculiar morphology.

Galaxy NGC 4650A (Fig. 2) is a prototype of PRGs with an extraordinary extended PR (Sersic 1967). Its structure was investigated in detail in many works (e.g., Gallagher et al. 2002; Iodice et al. 2002). As in the case of NGC 2685, the central galaxy of NGC 4650A looks like an edge-on S0 galaxy but just this galaxy has peculiar brightness distribution and colors. The ring, which is about 2–3 times the size of the central disk, is inclined with $\sim 100^{\circ}$ angle to the galaxy's major axis. The dark strip of absorption is visible at the place where ring is projected on the central galaxy. The ring itself has a complex structure: in the central part it is inclined to the line of sight and both parts are visible; however, at the distance of $30''$, they supposedly overlap when the ring is seen edge-on. Some of separate filaments are visible in the outer regions of the ring. According to Arnaboldi et al. (1997), the ring demonstrates some signs of spiral structure.

Data available in the literature concerning the color of NGC 2685 PR are inconsistent. In Hagen-Thorn et al. (1983) and Makarov et al. (1989), it has been shown, on the basis of *UBV* surface photometry, that a color of the ring is typical for the spiral arms of Sb–Sc galaxies. Peletier & Christodoulou (1993) found later that rings color is close to that of central galaxy, i.e., is red. However, this result is unclear due to the uncertainty of transformation of their *J* and *F* magnitude to the standard Johnson *BV* magnitude photometric system without taking into account the large radiation contribution of the emission lines.

The color of NGC 4650A PR is blue: $B-V \sim -0.1$ mag, according to Schechter et al. (1984), or $B-V \sim 0.2$–0.3 mag, according to Iodice et al. (2002).

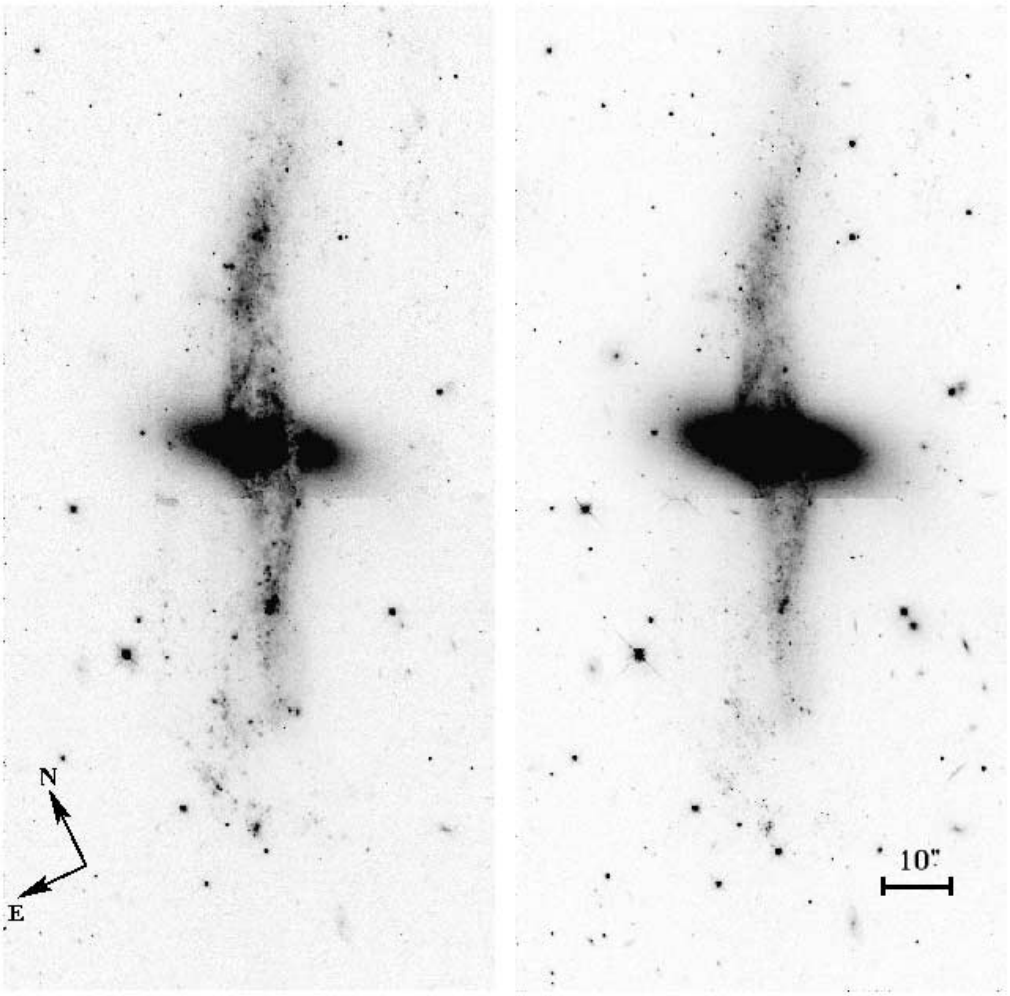

FIG. 2.—WFPC2 images of NGC 4650A (chips WF3 and WF4). *Left*, F450W-band image; *right*, F814W-band image. The blue color of the ring is evident.

Both galaxies were observed in the CO line $J = 2–1$ (Watson, Guptill, & Buchhilz 1994; Schinnerer & Scoville 2002). It is established that the emission is associated solely with the PRs. Watson et al. (1994) claimed that in NGC 4650A the mass of H_2 was 17%–35% of the H I mass, while in NGC 2685 this value exceeded the H I mass. However, Schinnerer & Scoville (2002) have found that Watson et al. (1994) overestimated the H_2 mass in NGC 2685 by an order of magnitude. Nevertheless, both galaxies have sufficient molecular clouds for star-forming activity.

There are some papers containing the claims on stellar populations and therefore the ages of PRs (Peletier & Christodoulou 1993; Iodice et al. 2002; Gallagher et al. 2002). For all the cases, results of surface photometry were used. In Peletier & Christodoulou (1993), the age of the NGC 2685 ring was estimated as ~5–6 Gyr on the basis of its color (however, these data are uncertain, see above). As for NGC 4650A, the data on ring colors show that the young stellar population certainly exist. The detailed surface colorimetry of the galaxy was done by Iodice et al. (2002) and Gallagher et al. (2002). In the first paper, the ages of 1–3 Gyr for the central region of the host galaxy and less than 10^8 yr for PR were found, while Gallagher et al. (2002) claimed that the ages of the host galaxy and the ring are 3–5 Gyr and ~1 Gyr, correspondingly.

A study of different stellar populations of the PRs, using their CMDs, will cast light on the origin and evolution of PRGs. We made here the first attempt to investigate the stellar population of PRs in NGC 2685 and NGC 4650A in such a way.

2. OBSERVATIONS AND BASIC DATA PROCESSING

We make use of archival *HST*/WFPC2 data of NGC 2685 and NGC 4650A. The observations of NGC 2685 were carried out as part of proposal No. 6633 by Marcella Carollo in 1999 January. The data set consists of images in F450W, F555W, and F814W bands with total exposure times of 2300, 1000, and 730 s, respectively. The NGC 4650A data set is based on the 7500 s exposures in the F450W band, 4763 s in F606W, and 7600 s in F814W, which were gathered under proposal No. 8399 by Keith Noll in 1999 April.

Figure 2 presents F450W- and F814W-band images of NGC 4650A. The blue color of the ring is evident. While WF3 and WF4 chips of WFPC2 cover the most part of NGC 4650A PR, the southern part of NGC 2685 and its ring are missing in the WFPC2 data. Total size of the NGC 2685 according to RC3 is $4.'5 \times 2.'3$. At the distance of NGC 2685, $1''$ corresponds to about 60 pc. For NGC 4650A, $1''$ corresponds to about 170 pc.

The raw frames were processed with the standard WFPC2 pipeline. The data were extracted from the archive using the

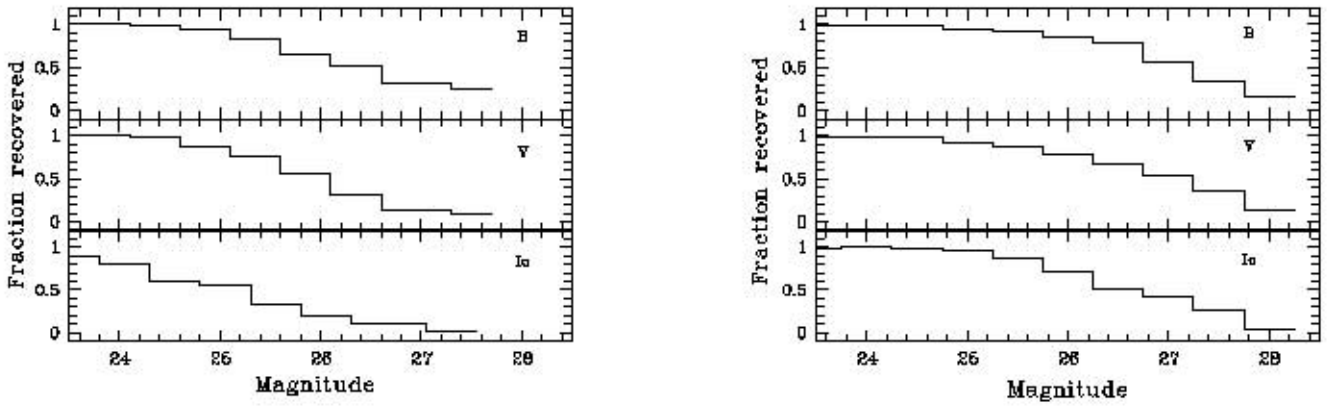

FIG. 3.—NGC 2685 (*left*) and NGC 4650A (*right*) completeness levels of the WFPC2 photometry based on artificial star tests

on-the-fly reprocessing STScI archive system, which reconstructs and calibrates original data with the latest calibration files, software, and data parameters. When it was possible, we used the recent version of the DITHERII package, which performs a "drizzling" (a variable pixel linear for correcting reconstruction) and corrects for geometric distortion. The processed frames were then separated into images for each individual CCD and trimmed of the vignetted regions using the boundaries recommended in the WFPC2 handbook. The images were combined after cleaning them for bad pixels and cosmic-ray events.

The single-star photometry of the images was processed with DAOPHOT/ALLSTAR. To avoid contamination by galactic background emission single-star photometry was performed on images with a subtracted median-smoothed (with a window of $10 \times$ FWHM) shape. The PSF was modeled and evaluated for each chip. The search of the stellar objects was made using the master frame produced from all images. The resulting list of stellar coordinates was given to ALLSTAR to perform the photometry in the individual frames. The necessary corrections were applied to resulting photometric data including a correction for charge-transfer inefficiency. The transformation from Holtzman et al. (1995) was used to convert instrumental magnitudes to the standard B (F450W), V (F555W, F606W), and I_C (F814W) system.

The F606W band is a wide "Hα continuum" and includes Hα. It may influence the accuracy of the NGC 4650A V-band photometry. Different band star lists were merged, requiring a positional source coincidence of better than $0.5 \times$ FWHM, or a box size of 2 pixels.

A completeness test was performed using the usual procedure of artificial star trials (Stetson 1994). A total of 1500 artificial stars were added to the F450W, F606W (F555W), and F814W band frames in several steps of 150 stars each. These had magnitudes and colors in the range 18.0 mag $\leq I_C \leq 28.0$ mag and 0.5 mag $\leq (V-I_C) \leq 1.5$ mag. Stars were considered to be recovered if they were found in all the bands with magnitudes not exceeding 0.75 mag brighter than the initial, injected ones. The results of the test are shown in Figure 3. As one can see in NGC 2685 the recovery is practically complete up to $m = 24.8$ mag in B band, $m = 24.6$ mag in V band and $m = 23.5$ mag in I_C band; for NGC 4650A up to $m = 25.6$ mag in the B band, $m = 25.2$ mag in the V band, and $m = 25.2$ mag in the I_C band. For more faint objects (within 1.0–1.5 mag) the recovering fraction is half as much.

3. RESULTS

There are ~450 stellar objects in NGC 4650A and ~800 in NGC 2685 detected in the B, V, and I_C filters with quality parameters SHARP and CHI (as defined in ALLSTAR in MIDAS) in the intervals $-1 \leq$ SHARP ≤ 1 and CHI ≤ 2. Our final lists of stellar objects include objects having angular sizes FWHM $< 0''.15$ for NGC 4650A and FWHM $< 0''.40$ for NGC 2685. Figure 4 illustrates the precision of our photometry.

The magnitudes and colors of these objects were corrected for extinction in our galaxy using *IRAS*/DIRBE map of Schlegel, Finkbeiner, & Davis (1998). With $R_V = 3.1$ and the extinction law of Cardelli, Clayton, & Mathis (1989), galactic foreground extinction for NGC 4650A is $A_B = 0.48$ mag, $A_V = 0.37$ mag, and $A_{I_C} = 0.22$ mag; and for NGC 2685 $A_B = 0.27$ mag, $A_V = 0.21$ mag, and $A_{I_C} = 0.12$ mag. The extinction-corrected data are used for construction of color-magnitude and color-color diagrams. The CMDs (B vs. $B-I_C$) for NGC 2685 and NGC 4650A are given in Figure 5.

Among the detected point objects, the bulk of which are evidently blue giants and supergiants, the outside objects with dimensions less than 25 pc may be present. The possible candidates are unresolved double and multiple stars, super–star clusters (SSCs) with typical dimensions of 8–10 pc, compact H II regions, and more extended H II regions with typical dimensions of about 20 pc.

It is difficult to separate multiple stars from single supergiants in our data, but the portion of systems in which the single blue supergiant is not dominant is probably not high (see below). There are no SSCs among our objects. Having mean absolute magnitudes of $M_V = -13$ mag (Whitmore et al. 1993), SSCs at the distance of NGC 2685 ($m - M = 30.5$ mag) will have an apparent magnitude of 17.5 and 19.7 mag at the distance of NGC 4650A ($m - M = 32.7$ mag). There are no such bright objects among those listed. H II regions can be separated using two-color diagrams. Since the Hα emission penetrates to the F606W band, the $V-I_C$ color for the H II regions proves to be less than one for blue stars ($V-I_C \sim -0.35$ mag). Therefore, H II regions have bluer color in $V-I_C$ than in $B-I_C$. As a result, all questionable objects were excluded from the final lists, which contained 430 stars for NGC 4650A and 800 stars for NGC 2685.

3.1. *NGC 2685*

In Figure 6 (*left*) the location of the blue (*circles*) and red (*squares*) supergiants of NGC 2685 is shown. It is evident that

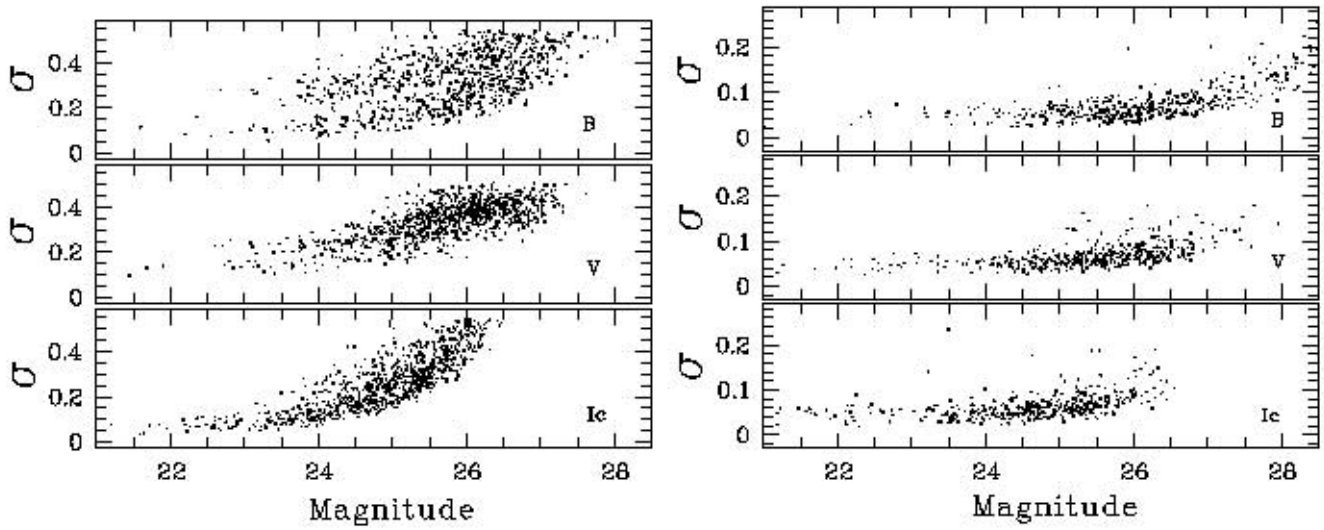

FIG. 4.—NGC 2685 (*left*) and NGC 4650A (*right*) errors of the WFPC2 photometry

the majority of both objects are concentrated to the region of PRs (although some objects in the lower right corner, perhaps, belong to the outer ring).

In the Figure 6 (*right*), we give an enlarged scale map of the portion of the galaxy near the PR; circles denote the most blue regions found after dividing frame F814W by F550W. All of these coincide with H II regions. Comparing the left and right panels of Figure 6, the correlation between locations of H II regions and blue supergiants is evident.

As one can see in the Figure 6, the amount of red supergiants is quite small. It is noticeable that both red and blue supergiants tend to gather into stellar associations. This fact also confirms that the detected stars are red supergiants of the PR rather than foreground Galactic red stars.

In the CMD B versus $B-I_C$ (Fig. 5), the blue limit of the stars is shifted to the red in comparison with normal position for blue supergiants which can be found from Bertelli et al. (1994). This points to significant intrinsic absorption in the PRs.

Comparison of the blue limit of the stars for the galaxy with that found for galaxies without intrinsic absorption gives the color excess for the galaxy. However, the blue limit at the CMDs is not sharp because of the different absorption for various stars and their different ages and metallicity. Therefore, it is more reliable to use the color index, for which the maximum in number of blue stars is observed, as a comparative parameter (this value gives the mean color index for blue supergiants and may be found after constructing the corresponding histogram).

For NGC 2685 $(B-I_C)^{\max} = +0.25$ mag; the comparison with galaxies NGC 959 $[(B-I_C)^{\max} = -0.18$ mag] and Holmberg II $[(B-I_C)^{\max} = -0.10$ mag] (our unpublished data; both galaxies may be considered as galaxies with negligible intrinsic absorption) gives $E_{(B-I_C)} = 0.39$ mag.

There is direct determination of absorption in the rings obtained from the surface photometry (Hagen-Thorn et al. 1983). It is known that the northeastern part of the main body

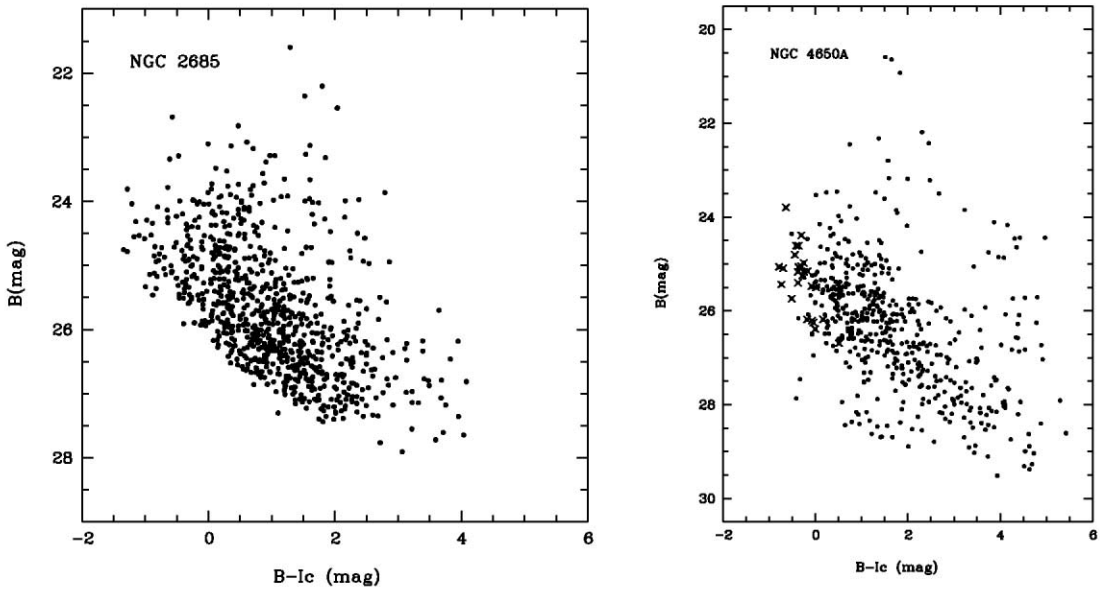

FIG. 5.—CMDs for NGC 2685 (*left*) and NGC 4650A (*right*) corrected for absorption in our Galaxy (crosses are unresolved H II regions)

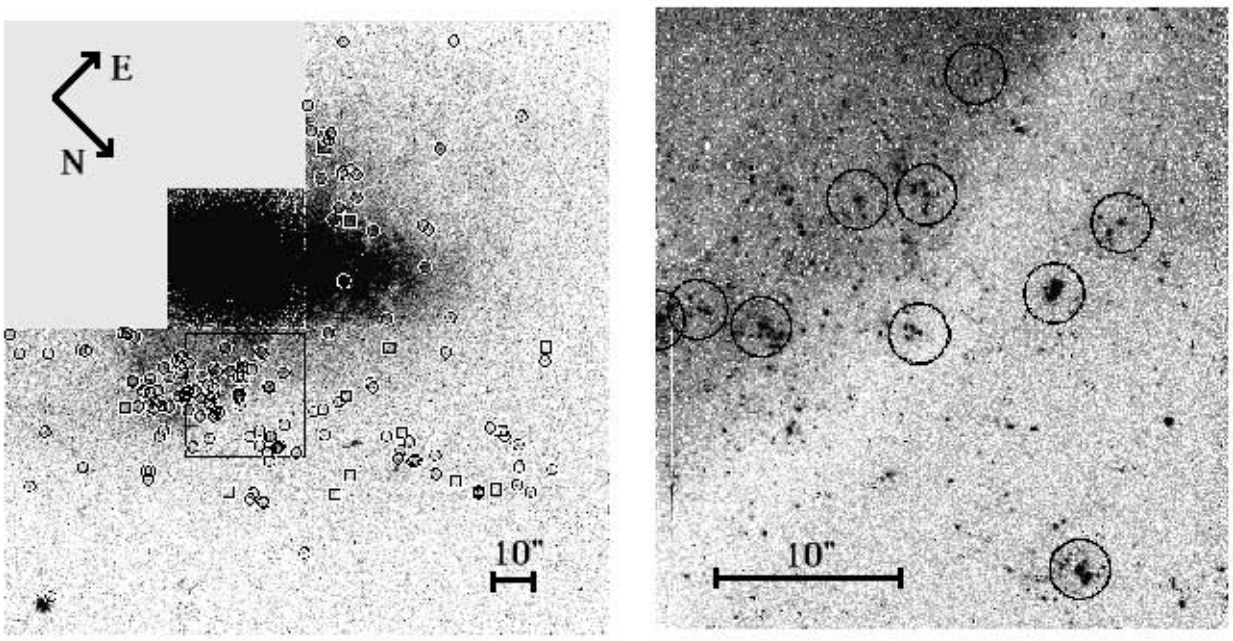

FIG. 6.—WFPC2 image of NGC 2685. Circles and squares indicate the position of blue and red supergiants, respectively (*left*). The H II region candidates to in the enlarged part of NGC 2685 PR (*right*).

of the galaxy is intersected by four dark strips for which the absorption was found (see Hagen-Thorn et al. 1983). These strips are the result of projection on the main body of PRs, which are luminous outside the galaxy (they simply follow each other). For a normal extinction curve (Cardelli et al. 1989) and a mean value of absorption in the B band for all four strips, one can find $E_{(B-I_C)} = 0.35$ mag.

The total absorption in several H II regions was obtained by Eskridge & Pogge (1997) on the basis of the Balmer decrement. The authors found that absorption A_V is essentially different in different H II regions (from 0.00 to 0.77 mag). After correction for galactic extinction, it gives $E_{(B-I_C)} = 0.40$ mag for the most obscured H II regions.

Two latter estimations do not contradict the value $E_{(B-I_C)} = 0.39$ mag found above. Therefore, we accept this. Since there is no possibility of correcting the data of individual stars for intrinsic absorption, we take it into account *in average*, reducing the color index $B-I_C$ for all stars by 0.39 mag and the magnitudes B, V, and I_C by 0.74, 0.56, and 0.35 mag, respectively.

The resulting M_{I_C} versus $B-I_C$ diagram (for $m - M = 30.5$ mag) is shown in Figure 7 (*left*).

3.2. *NGC 4650A*

In the CMD for NGC 4650A (Fig. 5), the crosses denote unresolved H II regions selected using two-color diagram. They have been excluded from the final list.

The location of detected blue stars in the field of NGC 4650A is shown in Figure 8 (*left*). The blue objects are evidently concentrated in the PR. Note that some stars follow so-called spiral arms (Arnaboldi et al. 1997; Gallagher et al. 2002), especially in their southern branch. As one can see in Figure 8 (*right*), red stars are distributed randomly without any concentration to the galaxy and are therefore foreground stars belonging to our Galaxy. (In NGC 4650A, we cannot reach the red giants that might form a halo around PR as the merging scenario demands.)

A comparison of the distribution of blue objects with the Hα image of the galaxy (Eskridge & Pogge 1999) shows (as in the case of the NGC 2685) a correlation between the location of the H II regions and the blue stars.

It is difficult to correct for intrinsic absorption in this case. According to Gallagher et al. (2002) there is a dust ring in the center of the galaxy. Iodice et al. (2002) give $A_B = 1.54$ mag and $A_{I_C} = 1.00$ mag for the extinction in the place of the ring projection on the main body. These values may be considered as an upper limit of intrinsic absorption in the ring outside the main body in regions of dust ring. However, the extreme blue ring colors far off the galactic center show that the extinction is very small (if any) in these regions. We attempt to introduce the correction for intrinsic absorption as linear along the PR from the center to periphery but without success because the scatter in the CMD along $B-I_C$ axis has not decrease. Therefore, we did not apply any correction for intrinsic absorption, keeping in mind that in reality stars at CMD may be located more left.

The resulting M_{I_C} versus $B-I_C$ diagram (for $m - M = 32.7$ mag) is shown in Figure 7 (*right*).

4. DISCUSSION

The important argument that benefits the assumption that most of the objects are blue supergiants gives the construction of luminosity functions (LFs) for blue objects in both galaxies. The LF was calculated for all objects with $B-I_C < 0.8$ mag for NGC 4650A and $B-I_C < 1.2$ mag for NGC 2685 [taking into account its reddening of $E_{(B-I_C)} = 0.39$ mag] by counting stars lying inside a bin of 0.5 mag. The central value was varied in steps of 0.25 mag to reduce the dependence of our results on the particular choice of bin center. The results are given in Figure 9.

As it was shown by Freedman (1985), the slope of the LF for blue supergiants is similar for all spiral galaxies with mean value of about 0.6. The slope of LF in the bright part (where the completeness is close to 100%) is 0.62 ± 0.01 for NGC 4650A and 0.61 ± 0.02 for NGC 2685 (*dashed lines*, Fig. 9), being in agreement with the Freedman (1985) value. Thus the results show that the PRs contain young blue

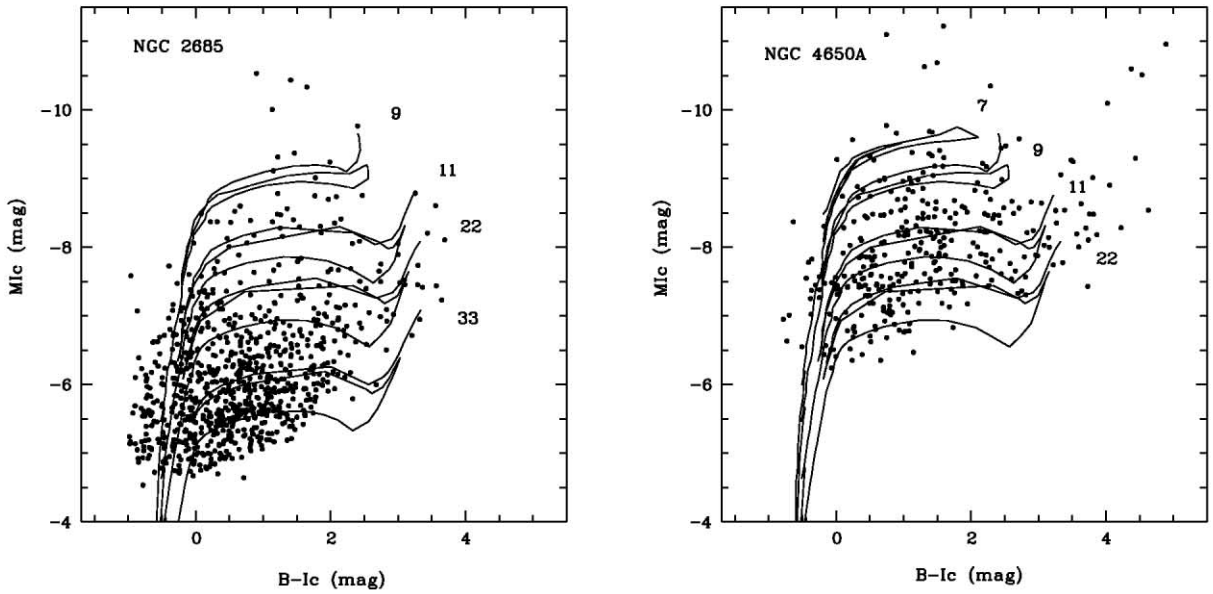

FIG. 7.—M_{I_C} vs. $B-I_C$ CMDs of NGC 2685 (*left*) and NGC 4650A (*right*). Stellar isochrones for the metallicity $Z = 0.008$ from the Padua library are overplotted for ages from 7 to 33 Myr.

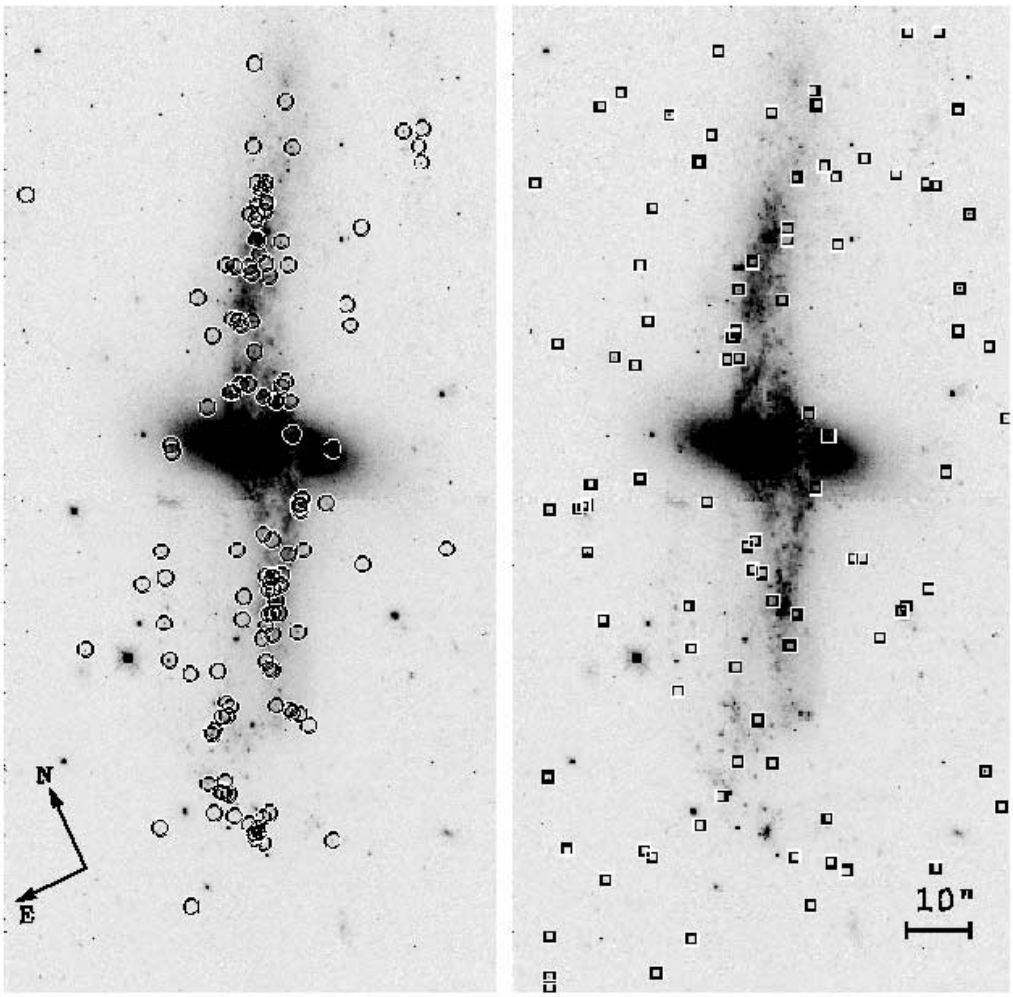

FIG. 8.—Blue supergiants (*circles*, *left*) in NGC 4650A and red stars (*squares*, *right*)

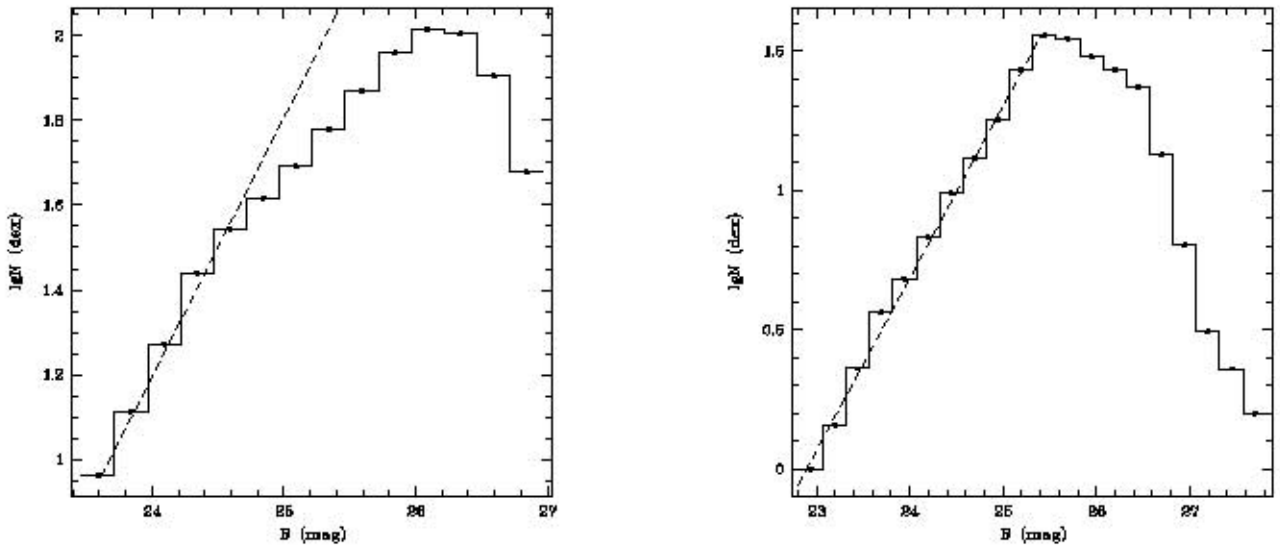

FIG. 9.—Smoothed LF of blue stars (*solid line*) and the bright-end slope of the LF (*dashed line*) of NGC 2685 (*left*) and NGC 4650A (*right*)

supergiants, testifying that star-forming processes are still going there.

The "color–absolute magnitude" diagrams for both galaxies presented in Figure 7 demonstrate mostly the brightest and youngest stellar populations. The CMD for NGC 2685 is deeper in comparison with that of NGC 4650A but still does not reach an area of old/intermediate-age stellar populations, for example, red giants ($M_{I_C} \approx -4.0$ mag). The discovery of red giants (old population) would allow us to estimate the age of the rings.

In Figure 7 the theoretical stellar isochrones from Bertelli et al. (1994) are overplotted for the metallicity of $Z = 0.008$ and ages from 7 to 33 Myr. Such a metallicity is usual for irregular galaxies (Garnett 2002). Isochrones for this metallicity are in good agreement with the CMDs observed by us. We do not find any confirmation of high metallicity in NGC 2685 as found by Eskridge & Pogge (1997), who used an empirical method for its determination, which strongly depends on accepted intrinsic absorption for H II regions. The isochrones for higher metallicity (e.g., solar) certainly contradict with the CMD observed.

From Figure 7, we can infer that the process of star formation was continuous during tens of megayears, and the last burst of star formation probably was more recent in NGC 4650A than in NGC 2685.

5. CONCLUSIONS

The main result of this work is the resolution of the PRs of NGC 2685 and NGC 4650A into stars. B, V, and I_C photometry was done for several hundreds of stars (mostly blue giants and supergiants) in each galaxy. Our research is the first one relating to resolvable stellar population in polar rings.

The distribution of blue and red supergiants in the field of galaxies strongly follows the PRs. The stars tend to gather into stellar associations which positions are correlated with positions of H II regions.

The CMDs for both galaxies show that process of star formation is continuous during tens of megayears, with the last burst of star formation being very recent (6.5 Myr in NGC 4650A and 9 Myr in NGC 2685). Unfortunately, the CMDs for both galaxies are insufficiently deep to claim anything about the old population in the rings. However, for NGC 2685 the upper limit of the red giant branch may be reached with deeper exposures with *HST* and planning such observations is very desirable. These observations might also verify whether a stellar halo exists around the main galaxy as predicted by Bournaud & Combes (2003) for the merging scenario of PRGs formation.

This work was supported by RFBR via grants 03-02-16344 and 02-02-16033.

REFERENCES

Arnaboldi, M., Freeman, K. C., Sackett, P. D., Sparke, L. S., & Capaccioli, M. 1995, Planet. Space Sci., 43, 1377
Arnaboldi, M., Oosterloo, T., Combes, F., Freeman, K. C., & Koribalski, B. 1997, AJ, 113, 585
Arp, H. C. 1966, Atlas of Peculiar Galaxies (Pasadena: Caltech)
Bekki, K. 1997, ApJ, 490, L37
Bertelli, G., Bressan, A., Choisi, C., Fagotto, F., & Nasi, E. 1994, A&AS, 106, 275
Bournaud, F., & Combes, F. 2003, A&A, 401, 817
Cardelli, J. A., Clayton, G. C., & Mathis, J. S. 1989, ApJ, 345, 245
Curir, A., & Diaferio, A. 1994, A&A, 285, 389
Eskridge, P. B., & Pogge, R. W. 1997, ApJ, 486, 259
———. 1999, in ASP Conf. Ser. 163, Star Formation in Early-Type Galaxies, ed. P. Carral & J. Cepa (San Francisco: ASP), 197
Freedman, W. L. 1985, ApJ, 299, 74
Gallagher, J. S., Sparke, L. S., Matthews, L. D., English, J., Kinney, A. L., Iodice, E., & Arnaboldi, M. 2002, ApJ, 568, 199
Garnett, D. 2002, ApJ, 581, 1019
Hagen-Torn, V. A., Popov, I. I., & Yakovleva, V. A. 1983, Astrofizika, 19, 599
Holtzman, J. A., Burrows, C. J., Casertano, S., Hester, J. J., Trauger, J. T., Watson, A. M., & Worthey, G. 1995, PASP, 107, 1065
Iodice, E., Arnaboldi, M., De Lucia, G., Gallagher, J. S., Sparke, L. S., & Freeman, K. C. 2002, AJ, 123, 195
Karataeva, G. M., Yakovleva, V. A., Hagen-Thorn, V. A., & Mikolaichuk, O. V. 2001, Astron. Lett., 27, 74
Makarov, V. V., Reshetnikov, V. P., & Yakovleva, V. A. 1989, Astrofizika, 30, 15
Peletier, R. F., & Christodoulou, D. M. 1993, AJ, 105, 1378
Reshetnikov, V. P., & Combes, F. 1994, Violent Star Formation From 30 Dorades to QSOs, ed. Tenorio-Tagle (Cambridge: Cambridge Univ. Press), 258
Richter, O.-G., Sackett, P. D., & Sparke, L. S. 1994, AJ, 107, 99
Sandage, A. R. 1961, The Hubble Atlas of Galaxies (Washington: Carnegie Inst.)
Schechter, P. L., & Gunn, J. E. 1978, AJ, 83, 1360
Schechter, P. L., Ulrich, M.-E., & Boksenberg, A. 1984, ApJ, 277, 526

Schinnerer, E., & Scoville, N. 2002, ApJ, 577, L103
Schlegel, D. J., Finkbeiner, D. P., & Davis, M. 1998, ApJ, 500, 525
Schweizer, F., Whitmore, B. C., & Rubin, V. C. 1983, AJ, 88, 909
Sersic, J. L. 1967, Z. Astrophys., 67, 306
Sersic, J. L., & Aguero, E. L. 1972, Ap&SS, 19, 387
Shane, W. W. 1980, A&A, 82, 314
Stetson, P. B. 1994, PASP, 106, 250
Tolstoy, E. 1999, in IAU Symp. 192, The Stellar Content of Local Group Galaxies, ed. P. Whitelock & R. Cannon (San Francisco: ASP), 218
Toomre, A. 1977, The Evolution of Galaxies and Stellar Populations, ed. R. B. Larson & B. M. Tinsley (New Haven: Yale Univ. Obs.), 418
van Driel, W., et al. 1995, AJ, 109, 942
Watson, D. M., Guptill, M. T., & Buchhilz, L. M. 1994, ApJ, 420, L21
Whitmore, B. C., Lucas, R. A., McElroy, D. B., Steiman-Cameron, T. Y., Sackett, P. D., & Olling, R. P. 1990, AJ, 100, 1489
Whitmore, B. C., Schweizer, F., Leitherer, C., Borne, K., & Robert, C. 1993, AJ, 106, 1354